arise from the different constraints imposed on the system, so that only experimental data can help in selecting the true Saha equation. Moreover, also accepting the maximization entropy criterion, we can have different formulations of the Saha equation depending on the definition of the relevant excitation temperatures, and these depend on the role of electrons and heavy particles in the dissociation and ionization processes.[23–27]

Conclusions

We have presented new calculations of thermodynamic and transport properties of equilibrium and nonequilibrium H_2 plasmas. In general, our results are in good agreement with those obtained by other authors.[16,21,22] The main conclusion that can be drawn from the results is that the thermodynamic and transport properties of two-temperature plasmas may depend in a nonnegligible manner on the adopted form of the Saha equation, which, in turn, is determined by the physical constraints imposed on the considered system.

Acknowledgment

This work has been supported by Agenzia Spaziale Italiana (Contracts I/R/163/00 and I/R/038/01).

References

[1]Giordano, D., "Thermodynamic Equilibrium of Multi-Temperature Gas Mixtures," *Molecular Physics and Hypersonic Flows*, edited by M. Capitelli, Kluwer Academic, Dordrecht, The Netherlands, 1996, pp. 259–280.

[2]Giordano, D., "Equivalence of Energy, Entropy, and Thermodynamic Potentials in Relation to the Thermodynamic Equilibrium of Multi-Temperature Gas Mixtures," *Physical Review E*, Vol. 58, 1998, pp. 3098–3112.

[3]Giordano, D., and Capitelli, M., "Two-Temperature Saha Equation: A Misunderstood Problem," *Journal of Thermophysics and Heat Transfer*, Vol. 9, No. 4, 1995, pp. 803, 804.

[4]Tisza, L., *Generalized Thermodynamics*, MIT Press, Cambridge, MA, 1977, pp. 245–287.

[5]Callen, H., *Thermodynamics*, Wiley, New York, 1963, pp. 295–331.

[6]Callen, H., *Thermodynamics and an Introduction to Thermostatics*, Wiley, New York, 1985.

[7]Napolitano, L., *Thermodynamique des Systems Composites en Equilibre ou Hors d'Equilibre*, Gauthier–Villars Editeurs, Paris, 1971, pp. 71–83.

[8]Potapov, A. V., "Chemical Equilibrium of Multitemperature Systems," *High Temperature (USSR)*, Vol. 4, No. 1, 1966, pp. 55–58.

[9]Veis, S., "The Saha Equation and Lowering of the Ionization Energy for a Two Temperature Plasma," *Proceedings of the Czechoslovak Conference on Electronics and Vacuum Physics*, Prague, 1968, pp. 105–109.

[10]Bose, T. K., "Thermophysical and Transport Properties of Multi-Component Gas Plasam at Multiple Temperatures," *Progress in Aerospace Sciences*, Vol. 25, 1988, pp. 1–42.

[11]Van de Sanden, M. C. M., Schram, P. P. J. M., Peeters, A. G., van der Mullen, J. A. M., and Kroesen, G. M. W., "Thermodynamic Generalization of the Saha Equation for a Two-Temperature Plasma," *Physical Review A: General Physics*, Vol. 40, No. 9, 1989, pp. 5273–5276.

[12]Morro, A., and Romeo, M., "On the Law of Mass Action in Fluid Mixtures with Several Temperatures," *Nuovo Cimento*, Vol. 7, No. 4, 1986, p. D539.

[13]Morro, A., and Romeo, M., "Thermodynamic Derivation of Saha's Equation for a Multi-Temperature Plasma," *Journal of Plasma Physics*, Vol. 39, No. 1, 1988, p. 41.

[14]Capitelli, M., and Molinari, E., "Problems of Determination of High Temperature Thermodynamic Properties of Rare Gases with Application to Mixtures," *Journal of Plasma Physics*, Vol. 4, No. 2, 1970, pp. 335–355.

[15]Capitelli, M., "Transport Properties of Partially Ionized Gases," *Journal de Physique* (Paris), Vol. C3-38, 1977, pp. 227–237.

[16]Aubreton, J., Elchinger, M. F., and Fauchais, P., "New Method to Calculate Thermodynamic and Transport Properties of a Multi-Temperature Plasma: Application to N_2 Plasma," *Plasma Physics and Plasma Processing*, Vol. 18, No. 1, 1998, pp. 1–27.

[17]Gorse, C., and Capitelli, M., "Collision Integrals of High Temperature Hydrogen Species," *Atomic and Plasma Data for Fusion (Supplement of Nuclear Fusion)* (to be published).

[18]Mason, E. A., Munn, R. J., and Smith, F. J., "Transport Coefficients of Ionized Gases," *Physics of Fluids*, Vol. 10, 1967, pp. 1827–1832.

[19]Capitelli, M., Colonna, G., Gorse, C., Minelli, P., Pagano, D., and Giordano, D., "Thermodynamic and Transport Properties of Two-Temperature H_2 Plasmas," AIAA Paper 2001-3018, June 2001.

[20]Capitelli, M., Ficocelli, E., and Molinari, E., "Equilibrium Compositions and Thermodynamic Properties of Mixed Plasmas: III–Argon–Hydrogen Plasmas at 10^{-2}–10^{3} Atmospheres Between 2,000 K and 35,000 K," Centro di Studio per la Chimica dei Plasmi, Istituto di Chimica Generale ed Inorganica, Univ. degli Studi, Bari, Italy, 1972.

[21]Murphy, A. B., "Transport Coefficients of Hydrogen and Argon–Hydrogen Plasmas," *Plasma Chemistry and Plasma Processing*, Vol. 20, No. 3, 2000, pp. 279–297.

[22]Devoto, R. S., "Transport Coefficients of Partially Ionized Gases," *Journal of Plasma Physics*, Vol. 2, No. 1, 1968, pp. 617–631.

[23]Tanaka, Y., Yokomizu, Y., Ishikawa, M., and Matsunura, T., "Particle Composition of High Pressure SF_6 Plasma with Electron Temperature Greater Than Gas Temperature," *IEEE Transactions on Plasma Science*, Vol. 25, No. 5, 1997, pp. 991–995.

[24]Girard, R., Belhaouuri, J. B., Gonzalez, J. J., and Gleizes, A., "A Two Temperature Kinetic Model of SF_6 Plasma," *Journal of Physics D: Applied Physics*, Vol. 32, No. 22, 1999, pp. 2890–2901.

[25]Gleizes, A., Chervy, B., and Gonzalez, J. J., "Calculation of a Two-Temperature Plasma Composition: Bases and Application to SF_6," *Journal of Physics D: Applied Physics*, Vol. 32, No. 16, 1999, pp. 2060–2067.

[26]Cliteur, C. J., Suzuki, K., Tanaka, Y., Sakuta, T., Matsubara, T., Yokomizu, Y., and Matsumura, T., "On the Determination of the Multi-Temperature SF_6 Plasma Composition," *Journal of Physics D: Applied Physics*, Vol. 32, No. 15, 1999, pp. 1851–1856.

[27]Miller, S. A., and Martinez-Sanchez, M., "Two-Fluid Nonequilibrium Simulation of Hydrogen Arcjet Trusters," *Journal of Propulsion and Power*, Vol. 12, No. 1, 1996, pp. 112–119.

Extended Slip Boundary Conditions for Microscale Heat Transfer

Yildiz Bayazitoglu* and Gokturk Tunc†
Rice University, Houston, Texas 77005

Nomenclature

Kn	=	Knudsen number
T	=	temperature, K
u_s	=	slip velocity, m/s
y	=	coordinate axis

Introduction

THE commonly used slip boundary conditions in microchannels are called the Maxwellian conditions, and they are first-order accurate in Knudsen number. In the present analysis, we develop the extended slip boundary conditions in a systematic manner to be used beyond the slip flow regime. The results are valid for early transition flows.

Analysis

A. Velocity Slip

When a gas flows over a surface, the molecules leave some of their momentum and create the shear stress on the wall. This momentum is the difference between the momentum of the incoming, M_{in}, and the reflected, M_{out}, molecules. The incoming momentum has two components: momentum of the impinging and the slipping molecules. The momentum going away from the surface is by reflection. As shown in Fig. 1, the specular reflection conserves the tangential momentum of the molecules $M_{specular} = M_{in}$, and the diffuse

Received 5 February 2002; accepted for publication 25 March 2002.

*H. S. Cameron Chair Professor, Mechanical Engineering and Materials Science Department, 6100 Main Street. Member AIAA.

†Graduate Student, Mechanical Engineering and Materials Science Department, 6100 Main Street.

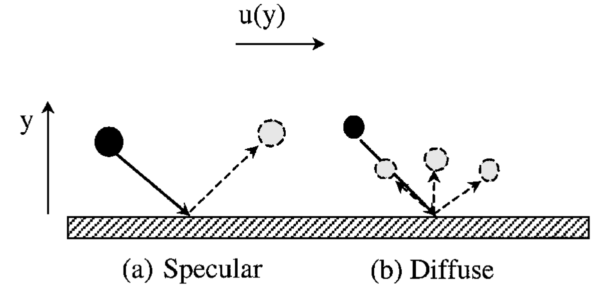

Fig. 1 Molecular reflection at the boundary.

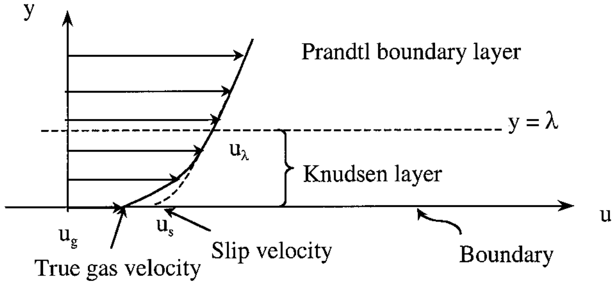

Fig. 2 Schematic of the velocity profile.

reflection results in vanishing tangential momentum, $M_{\text{diffuse}} = 0$. The fraction of the molecules that are diffusely reflected by the wall is defined as the tangential momentum accommodation coefficient F_m. When these definitions are used, the momentum leaving the surface can be written as

$$M_{\text{out}} = (1 - F_m) M_{\text{in}} \tag{1}$$

This results in the following wall momentum balance:

$$M_{\text{wall}} = F_m M_{\text{in}} \tag{2}$$

where the shear stress at the wall is given by $M_{\text{wall}} = \mu(\mathrm{d}u/\mathrm{d}y)_0$ and the incoming momentum is given by $M_{\text{in}} = \frac{1}{2}\mu(\mathrm{d}u/\mathrm{d}y)_0 + \frac{1}{2}\rho u_m u_0$. The first term is the momentum brought by the incoming stream, and the second term is due to the slip motion.[1] Figure 2 shows the Knudsen layer next to the boundary. We will evaluate Eq. (2) at this layer thickness λ as

$$\mu\left(\frac{\mathrm{d}u}{\mathrm{d}y}\right)_\lambda = F_m\left[\frac{1}{2}\mu\left(\frac{\mathrm{d}u}{\mathrm{d}y}\right)_\lambda + \frac{1}{2}\rho u_m u_\lambda\right] \tag{3}$$

Equation (3) is solved for the velocity at $y = \lambda$ as

$$u_\lambda = \frac{2 - F_m}{F_m}\lambda\left(\frac{\mathrm{d}u}{\mathrm{d}y}\right)_\lambda \tag{4}$$

where λ is the molecular mean free path and is defined as $\lambda = 2\mu/\rho u_m$, where μ is the dynamic viscosity, ρ is the density, and u_m is the mean velocity.

Maxwell's slip boundary condition has been applied routinely in the slip flow regime and has generated satisfactory results.[2,3] However, as Knudsen number Kn increases, the results of this boundary condition deviate from the Boltzmann solution. We propose the following representation of the velocity gradient at the wall. This approach is different from Beskok and Karniadakis's[4] approach in which they expanded the velocity at $y = \lambda$ around the wall instead of the velocity gradient. Therefore, we call the proposed relation the stress boundary condition and Beskok and Karniadakis's[4] approach the velocity boundary condition.

The velocity gradient at $y = \lambda$ is expanded around $y = 0$ as

$$\left(\frac{\mathrm{d}u}{\mathrm{d}y}\right)_\lambda = \left(\frac{\mathrm{d}u}{\mathrm{d}y}\right)_0 + \lambda\left(\frac{\mathrm{d}^2u}{\mathrm{d}y^2}\right)_0 + \frac{\lambda^2}{2}\left(\frac{\mathrm{d}^3u}{\mathrm{d}y^3}\right)_0 + \frac{\lambda^3}{6}\left(\frac{\mathrm{d}^4u}{\mathrm{d}y^4}\right)_0 + \cdots \tag{5}$$

Substituting Eq. (5) into Eq. (4) yields

$$u_s = \frac{2 - F_m}{F_m}\lambda\left[\left(\frac{\mathrm{d}u}{\mathrm{d}y}\right)_0 + \lambda\left(\frac{\mathrm{d}^2u}{\mathrm{d}y^2}\right)_0 + \frac{\lambda^2}{2}\left(\frac{\mathrm{d}^3u}{\mathrm{d}y^3}\right)_0 + \frac{\lambda^3}{6}\left(\frac{\mathrm{d}^4u}{\mathrm{d}y^4}\right)_0 + \cdots\right] \tag{6}$$

Equation (6) is nondimensionalized by $u^* = u/u_m$, $\eta = y/\ell$, and $Kn = \lambda/\ell$, where ℓ is the characteristic length, for example, the channel height, and obtained in the following form (note that superscript $*$ is dropped from the equations):

$$u_s = \frac{2 - F_m}{F_m}Kn\left[\left(\frac{\mathrm{d}u}{\mathrm{d}\eta}\right)_0 + Kn\left(\frac{\mathrm{d}^2u}{\mathrm{d}\eta^2}\right)_0 + \frac{Kn^2}{2}\left(\frac{\mathrm{d}^3u}{\mathrm{d}\eta^3}\right)_0 + \frac{Kn^3}{6}\left(\frac{\mathrm{d}^4u}{\mathrm{d}\eta^4}\right)_0 + \cdots\right] \tag{7}$$

Further rearrangement of the terms results in

$$u_s = \frac{2 - F_m}{F_m}Kn\left(\frac{\mathrm{d}u}{\mathrm{d}\eta}\right)_0\left\{1 + Kn\left[\frac{(\mathrm{d}^2u/\mathrm{d}\eta^2)_0}{(\mathrm{d}u/\mathrm{d}\eta)_0}\right] + \frac{Kn^2}{2}\left[\frac{(\mathrm{d}^3u/\mathrm{d}\eta^3)_0}{(\mathrm{d}u/\mathrm{d}\eta)_0}\right] + \frac{Kn^3}{6}\left[\frac{(\mathrm{d}^4u/\mathrm{d}\eta^4)_0}{(\mathrm{d}u/\mathrm{d}\eta)_0}\right] + \cdots\right\} \tag{8}$$

Next, we introduce the asymptotic expansion

$$1\bigg/\left[1 - Kn\left(\frac{\mathrm{d}^2u/\mathrm{d}\eta^2}{\mathrm{d}u/\mathrm{d}\eta}\right)_0\right] = 1 + Kn\left(\frac{\mathrm{d}^2u/\mathrm{d}\eta^2}{\mathrm{d}u/\mathrm{d}\eta}\right)_0 + Kn^2\left(\frac{\mathrm{d}^2u/\mathrm{d}\eta^2}{\mathrm{d}u/\mathrm{d}\eta}\right)_0^2 + Kn^3\left(\frac{\mathrm{d}^2u/\mathrm{d}\eta^2}{\mathrm{d}u/\mathrm{d}\eta}\right)_0^3 + \cdots \tag{9}$$

to Eq. (8) and organize the resulting expression as

$$u_s = \frac{2 - F_m}{F_m}Kn\left(\frac{\mathrm{d}u}{\mathrm{d}\eta}\right)_0\left[1\bigg/\left[1 - Kn\left(\frac{\mathrm{d}^2u/\mathrm{d}\eta^2}{\mathrm{d}u/\mathrm{d}\eta}\right)_0\right] + \frac{Kn^2}{2}\left(\frac{\mathrm{d}^3u/\mathrm{d}\eta^3}{\mathrm{d}u/\mathrm{d}\eta}\right)_0 + \frac{Kn^3}{6}\left(\frac{\mathrm{d}^4u/\mathrm{d}\eta^4}{\mathrm{d}u/\mathrm{d}\eta}\right)_0 + \cdots - \left(Kn\frac{\mathrm{d}^2u/\mathrm{d}\eta^2}{\mathrm{d}u/\mathrm{d}\eta}\right)_0^2 - \left(Kn\frac{\mathrm{d}^2u/\mathrm{d}\eta^2}{\mathrm{d}u/\mathrm{d}\eta}\right)_0^3 - \left(Kn\frac{\mathrm{d}^2u/\mathrm{d}\eta^2}{\mathrm{d}u/\mathrm{d}\eta}\right)_0^4 - \cdots\right] \tag{10}$$

or simply

$$u_s = \frac{2 - F_m}{F_m}\frac{Kn}{1 - bKn}\left(\frac{\mathrm{d}u}{\mathrm{d}\eta}\right)_0 + \text{res} \tag{11}$$

where $b = (\mathrm{d}^2u/\mathrm{d}\eta^2)/(\mathrm{d}u/\mathrm{d}\eta)$ and the residual is given by

$$\text{res} = \frac{2 - F_m}{F_m}\left[\frac{Kn^3}{2}\left(\frac{\mathrm{d}^3u}{\mathrm{d}\eta^3}\right)_0 + \frac{Kn^4}{6}\left(\frac{\mathrm{d}^4u}{\mathrm{d}\eta^4}\right)_0 + \frac{Kn^5}{24}\left(\frac{\mathrm{d}^5u}{\mathrm{d}\eta^5}\right)_0 + \cdots - Kn^3\frac{(\mathrm{d}^2u/\mathrm{d}\eta^2)_0^2}{(\mathrm{d}u/\mathrm{d}\eta)_0} - Kn^4\frac{(\mathrm{d}^2u/\mathrm{d}\eta^2)_0^3}{(\mathrm{d}u/\mathrm{d}\eta)_0^2} - Kn^5\frac{(\mathrm{d}^2u/\mathrm{d}\eta^2)_0^4}{(\mathrm{d}u/\mathrm{d}\eta)_0^3} - \cdots\right] \tag{12}$$

For flow between two parallel plates, we have $\mathrm{d}^2u/\mathrm{d}\eta^2 = -2$ and $\mathrm{d}u/\mathrm{d}\eta = 1$. Therefore, the coefficient b is calculated to be equal to -2. The analysis of Ref. 4 using the velocity boundary condition obtained $b = -1$. The velocity boundary condition was first introduced by Schaaf and Chambre.[5] They took the slip velocity as the average of the tangential velocity of the approaching and the reflected molecules. They assumed that the velocity of approaching molecules is the same as the velocity on the Knudsen layer and, therefore, is the velocity of the specularly reflected molecules. They obtained the slip velocity as

$$u_s = \tfrac{1}{2}(u_{\mathrm{in}} + u_{\mathrm{out}}) = \tfrac{1}{2}[u_\lambda + (1 - F_m)u_\lambda] = [(2 - F_m)/2]u_\lambda \quad (13)$$

The velocity at $y = \lambda$ was written by expanding the velocity profile around $y = 0$. Beskok and Karniadakis[4] used the first two terms of this expansion and obtained the second-order slip boundary condition without the residual term with $b = \frac{1}{2}(\mathrm{d}^2u^*/\mathrm{d}\eta^2)_0/(\mathrm{d}u^*/\mathrm{d}\eta)_0$.

Figure 3 shows the slip velocity for three different analyses for $10^{-2} \leq Kn \leq 2$. The dashed line corresponds Beskok and Karniadakis's velocity boundary condition[4] and the solid line corresponds to the present stress boundary condition. The stress boundary condition provides better results than the velocity boundary condition compared to the linearized Boltzmann solution of Ohwada et al.[6]

Note that the resultant stress boundary condition can be used for only small Knudsen number Kn values, where the characteristic length is larger than the Knudsen layer. In addition to this physical limit, a mathematical lower limit is also introduced by the given asymptotic expansion. Assuming a parabolic velocity profile and using the values of the first- and second-order derivatives at the wall, we can write the residual as

$$\mathrm{res} = -\sum_{i=2}^{\infty} Kn^{i+1}(-2)^i$$

The residual is calculated for different values of Knudsen number Kn, and the resulting error values with respect to the calculated slip velocity are shown in Table 1. Negative values of the residual explain the overestimation of the slip velocity as shown in Fig. 3. Based on the error analysis, we can conclude that our approximation is valid up to Knudsen numbers around 0.5. This conclusion is consistent with the physical constraint of $Kn < 1$.

Table 1 Error generated from asymptotic expansion

Kn	Residual	u_s	% Error
0.0	0.0	0.0	0.0
0.1	−0.0033	0.3333	0.99
0.2	−0.0229	0.4615	4.9
0.3	−0.0675	0.5294	12.7
0.4	−0.1422	0.5714	24.88
0.5	0.0	0.6	0.0
0.6	-3.25×10^7	0.6207	∞

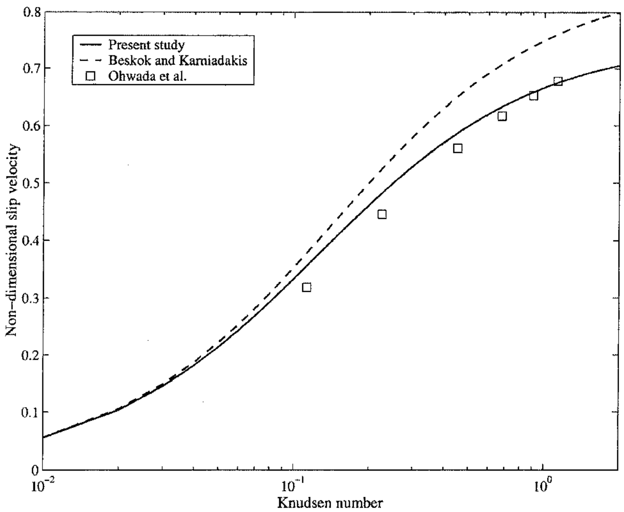

Fig. 3 Comparison of the slip velocity in $10^{-2} \leq Kn \leq 2$.

A similar boundary condition for a cylindrical pipe will now be derived. The velocity λ away from the surface is obtained as

$$u_{R-\lambda} = -\frac{2 - F_m}{F_m}\lambda\left(\frac{\mathrm{d}u}{\mathrm{d}y}\right)_{R-\lambda} \quad (14)$$

We expand the derivative around $r = R$, where R is the channel radius:

$$\left(\frac{\mathrm{d}u}{\mathrm{d}y}\right)_{R-\lambda} = \left(\frac{\mathrm{d}u}{\mathrm{d}y}\right)_R - \lambda\left(\frac{\mathrm{d}^2u}{\mathrm{d}y^2}\right)_R + \frac{\lambda^2}{2}\left(\frac{\mathrm{d}^3u}{\mathrm{d}y^3}\right)_R + \cdots \quad (15)$$

Equation (15) is substituted into Eq. (14), and the following expansion is utilized:

$$1\bigg/\left(1 + Kn\frac{\mathrm{d}^2u/\mathrm{d}\eta^2}{\mathrm{d}u/\mathrm{d}\eta}\right) = 1 - Kn\frac{\mathrm{d}^2u/\mathrm{d}\eta^2}{\mathrm{d}u/\mathrm{d}\eta} + Kn^2\left(\frac{\mathrm{d}^2u/\mathrm{d}\eta^2}{\mathrm{d}u/\mathrm{d}\eta}\right)^2 - Kn^3\left(\frac{\mathrm{d}^2u/\mathrm{d}\eta^2}{\mathrm{d}u/\mathrm{d}\eta}\right)^3 + \cdots \quad (16)$$

to obtain

$$u_s^* = -\frac{2 - F_m}{F_m}\frac{Kn}{1 + bKn}\left(\frac{\mathrm{d}u^*}{\mathrm{d}\eta}\right)_{\eta=1} \quad (17)$$

where

$$u^* = \frac{u}{u_m}, \qquad \eta = \frac{y}{R}, \qquad b = \frac{(\mathrm{d}^2u^*/\mathrm{d}\eta^2)_{\eta=1}}{(\mathrm{d}u^*/\mathrm{d}\eta)_{\eta=1}}, \qquad Kn = \frac{\lambda}{R}$$

The coefficient b is calculated as 1 for cylindrical geometry.

B. Temperature Jump

In this section, the derivation of temperature jump boundary condition as outlined by Kennard[1] will be presented. The derivation starts with the definition of the thermal accommodation coefficient as $F_T = (Q_i - Q_r)/(Q_i - Q_w)$. Q_i is the energy of the impinging molecules, Q_r is the energy carried by the reflected molecules, and Q_w is energy that the molecules would have if they left the wall at the wall temperature.

The numerator of this relation is the net heat transfer and is given by

$$Q_i - Q_r = k\left(\frac{\partial T}{\partial y}\right)_\lambda \quad (18)$$

and the denominator is obtained from

$$Q_i - Q_\lambda = m\left(c_v + \frac{1}{2}R\right)(T_s - T_\lambda) + \frac{1}{2}k\left(\frac{\partial T}{\partial y}\right)_\lambda \quad (19)$$

where the difference between the internal and kinetic energies of the approaching and reflected molecules is added to the heat conduction by the approaching molecules. In Eq. (19), m is the mass, c_v is the specific heat at constant volume, R is the gas constant, and k is the thermal conductivity. When the definition of F_T is used and the kinetic theory of gases is utilized, the temperature jump can be solved as

$$T_\lambda - T_w = \frac{2 - F_T}{F_T}\frac{2\gamma}{\gamma + 1}\frac{\lambda}{Pr}\left(\frac{\partial T}{\partial y}\right)_\lambda \quad (20)$$

where γ is the specific heat ratio. Equation (20) provides the first-order boundary condition if the temperature gradient at the wall is assumed to be the same as the one on $y = \lambda$. The second-order temperature jump boundary condition is obtained by following the approach applied in obtaining the velocity slip boundary condition as

$$\theta_s - \theta_w = \frac{2 - F_T}{F_T}\frac{2\gamma}{\gamma + 1}\frac{Kn}{Pr(1 - aKn)}\left(\frac{\partial\theta}{\partial\eta}\right)_0 \quad (21)$$

where Pr is the Prandtl number, θ is the nondimensional temperature, $\theta = T/T_{\mathrm{reference}}$, subscripts s and w correspond to the fluid temperature at the wall and the wall temperature, and $a = (\mathrm{d}^2\theta/\mathrm{d}\eta^2)_0/(\mathrm{d}\theta/\mathrm{d}\eta)_0$.

Conclusions

The velocity slip and temperature jump boundary conditions were derived for $Kn \le 0.5$. Velocity gradient on the wall was obtained from the expansion of the gradient on Knudsen layer unlike the previous analyses that used the expansion of velocity itself. The slip velocities calculated from the present stress boundary condition agreed well with the linearized Boltzmann results.

References

[1]Kennard, E. H., *Kinetic Theory of Gases*, McGraw–Hill, New York, 1938, pp. 295–315.

[2]Arkilic, E. B., Breuer, K. S., and Schmidt, M. A., "Gaseous Flow in Microchannels," *Application of Microfabrication to Fluid Mechanics*, FED Vol. 197, American Society of Mechanical Engineers, Fairfield, NJ, 1994, pp. 57–66.

[3]Harley, J. C., Huang, Y., Bau, H. H., and Zemel. J. N., "Gas Flow in Micro-Channels," *Journal of Fluid Mechanics*, Vol. 284, 1995, pp. 257–274.

[4]Beskok, A., and Karniadakis, G. E., "Models and Scaling Laws for Rarefied Internal Gas Flows Including Separation," 48th Annual Meeting of the American Physical Society Division of Fluid Dynamics, Nov. 1995.

[5]Schaaf, S. A., and Chambre, P. L., *Flow of Rarefied Gases*, Princeton Univ. Press, Princeton, NJ, 1961.

[6]Ohwada, T., Sone, Y., and Aoki, K., "Numerical Analysis of the Poiseuille and Thermal Transpiration Flows Between Two Parallel Plates on the Basis of the Boltzman Equation for Hard-Sphere Molecules," *Physics of Fluids A*, Vol. 1, No. 12, 1989, pp. 2042–2049.

Transient Coupled Radiation and Conduction in a Two-Layer Semitransparent Material

Ping-Yang Wang* and Hui-Er Cheng†
Shanghai Jiaotong University, 200030 Shanghai, People's Republic of China
and
He-Ping Tan‡
Harbin Institute of Technology, 150001 Harbin, People's Republic of China

Introduction

SEMITRANSPARENT material (STM), in which the nature of the radiative transfer can provide a positive or negative internal heat source, is widely applied to engineering. Recently, some researchers have focused on coupled radiation and conduction in a two-layer or multilayer planer STM, such as Ho and Özisik,[1] Spuckler and Siegel,[2] and Siegel.[3] The ray tracing/nodal analysis method was provided in Refs. 4 and 5 to obtain transient temperatures in a single-layer nonscattering STM and isotropically scattering STM, respectively. After that, Refs. 6 and 7 extended this method to a two-layer, isotropically scattering STM with the semitransparent or the opaque boundaries, respectively. Some conclusions were drawn, for example, when one side is heated and the other is cooled, the temperature maximums can appear inside the composite with both semitransparent boundaries[6]; however, for both opaque boundaries the temperature maximums only appear at the heated boundary.[7] The derivation of this method is extended here for a two-layer, isotropically scattering and nongray composite with one semitransparent boundary and one opaque boundary, and the emphasis is placed on investigating whether the peak value of temperature will appear inside the composite and the effects of refractive index and conduction-radiation parameter on temperature distribution. The nomenclature used herein is the same as that of Refs. 6 and 7.

Received 25 January 2001; revision received 28 January 2002; accepted for publication 19 March 2002.

*Postdoctor, Institute of Engineering Thermophysics, 1954 Huashan Road.

†Professor, Institute of Engineering Thermophysics, 1954 Huashan Road.

‡Professor, School of Energy Science and Engineering, 92 West Dazhi Street.

Analysis

A two-layer planar STM with one semitransparent boundary S_1 and one opaque boundary S_2, as shown in Fig. 1, is located between two black surfaces $S_{-\infty}$ and $S_{+\infty}$, which, respectively, denote the outside surroundings. The reflectivities of surfaces S_1, S_P, and S_2 are ρ_1, ρ_P, and ρ_2; the transmissivities of semitransparent surfaces S_1 and S_P are γ_1 and γ_P. The composite is divided into M control volumes. For this physical model the energy equation and the radiative heat source for the transient coupled radiation and conduction are the same as those in Ref. 5, but the radiative transfer coefficient (RTC) and the boundary conditions need to be rededuced. The RTC is defined as the total quotient of the radiative energy arriving at the investigated element in the transfer process and the radiative energy emitted by another one. The transfer process of radiative energy in a scattering STM can be divided into two subprocesses: a nonscattering subprocess and a scattering subprocess.[5] The derivation of scattering subprocess[5] is not provided here because it is independent of the radiative properties of the boundary surfaces. The notation for RTC given in Refs. 6 and 7 is still used, that is, $(S_u S_v)_k$, $(S_u V_j)_k$, and $(V_i V_j)_k$ denote RTCs of surface S_u transferring to surface S_v, surface S_u transferring to volume V_j, and volume V_i transferring to volume V_j for nonscattering materials, respectively; and $[S_u S_v]_k$, $[S_u V_j]_k$, and $[V_i V_j]_k$ denote RTCs for scattering materials. S_u and S_v denote surface $S_{-\infty}$ or S_2; V_i and V_j denote the ith and jth control volumes, respectively; and subscript k refers to the spectral band of interest.

Radiative Transfer Coefficient

Take $(S_{-\infty} V_j)_k$ as an example and assume that V_j belongs to the second layer. The deductive process used in determining the RTCs for diffuse reflection are provided here through tracing the radiative energy by using the philosophy of the ray tracing method in combination with the direct radiative transfer coefficient (DRTC). The DRTC is defined as the RTC not considering reflection and is denoted by $(s_w s_z)_k$, $(s_w v_j)_k$, and $(v_i v_j)_k$, whose equations are given in Ref. 7; s_w and s_z denote surfaces S_1, S_P, or S_2; and v_i and v_j denote control volumes V_i and V_j, respectively.

For the unit radiative energy that comes from $S_{-\infty}$, a part entering the composite through surface S_1 is absorbed by the first layer medium, then transmitted and reflected through surfaces S_1 and S_P. In the end it is attenuated to zero. In this transfer process

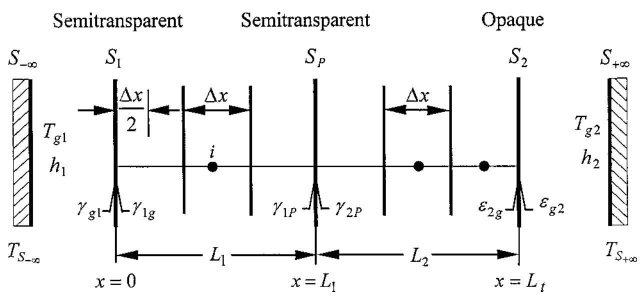

Fig. 1 Zonal discretization model of a two-layer planar composite medium.